Available online at www.sciencedirect.com
SCIENCE DIRECT
Biochemical Pharmacology 70 (2005) 47–58
Biochemical Pharmacology
www.elsevier.com/locate/biochempharm

Tamoxifen alters gating of the BK α subunit and mediates enhanced interactions with the avian β subunit

R.K. Duncan *

Kresge Hearing Research Institute, University of Michigan, 4036 KHRI, 1301 E. Ann Street, Ann Arbor, MI 48109-0506, USA

Received 5 January 2005; accepted 30 March 2005

Abstract

Mammalian BK channels are modulated by estrogen and non-steroidal estrogen-like compounds (i.e. xenoestrogens), but the effects are dependent on channel composition. (Xeno)estrogens preferentially activate BK channels through accessory β subunits, but reduce single-channel conductance by interaction with α subunits. In this report, the xenoestrogen tamoxifen was applied to chicken BK channels, in order to asses the mechanism behind drug interaction and to determine the extent to which (xeno)estrogen interaction is extended to avian BK homologs. As with mammalian isoforms, the properties of chicken BK channels were modulated by tamoxifen in a subunit-dependent manner. Tamoxifen reduced single-channel conductance through interaction with the α subunit. However, if the expression construct included the β subunit, tamoxifen increased the channel's open probability and shifted the voltage-activation range to more negative potentials. This effect on channel gating was concentration-dependent, with an EC_{50} of about 0.2 μM. Tamoxifen-mediated reductions in gating charge and in the intrinsic energetics that govern channel equilibrium. The relative contribution of these two effects on channel gating was altered by β co-expression. Modulation by (xeno)estrogens may be an evolutionarily conserved mechanism for non-genomic hormonal actions, and the limited conservation between avian and mammalian β subunits may suggest potential binding motifs. Alternatively, the data are consistent with a tamoxifen-mediated conformation change in the α subunit that alters the way α and β subunits interact, resulting in enhanced gating without direct binding to β.

Keywords: Calcium-activated potassium channel; Hormone; Estrogen; Xenoestrogen; Chicken

1. Introduction

In many excitable cells, large-conductance, Ca^{2+}-, and voltage-sensitive K^+ channels (BK) constrain calcium influx during stimulation, and this negative feedback influences a number of processes including cell excitability, neurotransmission, secretion, muscle contraction, and hearing [1–5]. This central role in calcium-triggered events has led to considerable interest in the normal biophysical properties of BK channels and in mechanisms for modulating their behavior [6]. Channel properties can be diversified by co-assembly with accessory proteins [7–11]. Of these accessory proteins, auxiliary β subunits have received the most attention, because they substantially alter BK channel gating properties [12] and pharmacology [13–15].

A family of four β subunit isoforms have been identified in human (β1–β4), each conferring specific biophysical properties to the BK channel [7]. Orthologs have been found for other mammalian species [16], and an avian homolog has been cloned from chicken and quail [17]. The topologies and functional effects of the avian β and mammalian β1 subunits are similar, even though sequence identity is low [18]. It remains to be seen whether the avian and mammalian homologs affect BK pharmacology in comparable ways.

The BK channel's response to toxins, kinases, and other modulators is largely dependent on subunit composition, and there is a growing appreciation for how β subunits can alter BK channel pharmacology [7]. Estrogen and xenoestrogens (i.e. non-steroidal estrogen-like compounds) exert genomic and non-genomic effects on cellular physiology [19–21], and one of the non-genomic, plasma membrane associated targets is the BK channel [22]. In heterologous expression of mammalian isoforms, BK channels were preferentially activated by the application of 17β-estradiol

* Present address: Department of Otolaryngology: Head and Neck Surgery, Johns Hopkins University, Baltimore, MD 21205, USA.
Tel.: +1 734 763 2129; fax: +1 734 764 0014.
E-mail address: rkduncan@umich.edu.

0006-2952/$ – see front matter © 2005 Elsevier Inc. All rights reserved.
doi:10.1016/j.bcp.2005.03.026

[22] or structurally related xenoestrogens [23–25], but these effects only occurred when channel constructs included both α and β1 subunits. It is unclear whether all members of the mammalian β subunit family behave similarly, but recent evidence suggests that 17β-estradiol also acts through the mammalian β4 subunit [26]. Surprisingly, the sequence identity between β1 and β4 subunits is poor (~22% amino acid identity) [26], limiting potential interaction motifs. Since conserved residues are generally shared with other β isoforms [17,26], the binding motif and steroid sensitivity may be conserved among all family members. Therefore, it was hypothesized that the xenoestrogen tamoxifen (Tx) would preferentially activate chicken homologs, when the channel included the cβ subunit.

Results indicated that avian and mammalian BK channels were modulated by Tx in similar ways. In addition, the results extended previous results by showing a voltage-dependent inhibition of BK channels through interaction with the α subunit alone. The conserved modulation of avian BK channels by (xeno)estrogens offers the potential for exploiting subunit-dependent pharmacology to determine molecular composition at the single-channel level [27]. An underlying rationale for this work is the desire to explore BK channel heterogeneity in the chicken cochlea, where graded expression of the BK β subunit has been implicated in the functional gradients that relate to sensory processing in that organ [18,28].

2. Materials and methods

2.1. Plasmid constructs and HEK transfection

BK channels were expressed in HEK293 cells using a calcium–phosphate transfection kit (Invitrogen, Carlsbad, CA) or through cationic-lipid-mediated transfection (Lipofectamine 2000, Invitrogen). Cells were propagated in high-glucose DMEM (Mediatech, Herndon, VA) with 6 mM L-glutamine and supplemented with 10% fetal bovine serum (Sigma, St. Louis, MO), 1% penicillin/streptomycin (Invitrogen), and 6.25 μg/ml Plasmocin (Invivogen, San Diego, CA). In some cases, Fungizone (Invitrogen) was added to growth media at 1.25 μg/ml to prevent contaminants. However, Fungizone was omitted from media during transfection, and recordings were made on cells incubated for at least 72 h without this antimycotic. The cells were maintained in a humidified atmosphere with 5% CO_2 at 37 °C. Cells were cycled through no more than six passages before fresh stocks were seeded. It should be noted that growth media included the pH-sensitive dye phenol red, which has been shown to act as a weak estrogen [29]. It is unlikely that phenolic compounds or endogenous serum estrogens competed with tamoxifen during experimental recordings, since (xeno)estrogen modulation is readily reversible (see Section 3) and growth media was exchanged with a phenol and serum free saline for at least 5 min prior to establishing BK recordings.

Plasmids for expression in mammalian cell lines were created by ligating full-length cDNA clones into pcDNA 3.1 (Invitrogen). The chicken α subunit, used throughout this paper, was the minimal variant described previously as α_0 or *cslo*1 [30,31] (accession number U23821). A clone of the chicken β subunit was generously provided by Corrina Oberst Sonderegger and Klaus Bister (accession number AF077369) and subcloned into pcDNA3.1 for heterologous expression. Transfection mixes included pEGFPLuc (BD Biosciences Clontech, Palo Alto, CA) for fluorescence detection of transfected cells.

2.2. Electrophysiology and recording solutions

Patch-clamp recordings were made 24–48 h after transfection. HEK cells, subcultured onto glass coverslips, were transferred to an inverted microscope with epi-fluorescence illumination. Growth media was exchanged with a high-Na^+ bath saline (154 mM NaCl, 6 mM KCl, 5 mM $CaCl_2$, 2 mM $MgCl_2$, 5 mM HEPES, buffered to pH 7.4 with NaOH) to facilitate seal formation. Microelectrodes were pulled from borosilicate glass capillaries (World Precision Instruments, Sarasota, FL) to a resistance between 5 and 10 MΩ and coated with ski-wax or Sylgard (World Precision Instruments) to reduce capacitance. Pipettes were filled with an internal solution consisting of 142 mM KCl, 0.5 mM $MgCl_2$, 5 mM HEPES, 2 mM diBr$_2$-BAPTA (Molecular Probes Inc., Eugene, OR), and enough $CaCl_2$ to give a free Ca^{2+} concentration of 1 μM. This Ca^{2+} concentration was set using a calcium electrode (Microelectrodes Inc., Bedford, NH) calibrated with multiple Ca^{2+} standards (World Precision Instruments). After forming a tight seal (>2 GΩ) to a GFP-positive cell, brief depolarizing voltage steps were applied in whole-cell recording mode. If fast, voltage-gated outward currents indicative of BK channels were evident, the pipette was gently moved away from the cell until an outside-out excised patch was obtained. The bath saline was exchanged for a high-K^+ control saline (142 mM KCl, 0.5 mM $MgCl_2$, 1.08 mM $CaCl_2$, 5 mM HEPES, 2 mM EGTA, buffered to pH 7.2 with KOH, giving 0.2 μM free Ca^{2+}) so that patches were exposed to isometric potassium. The internal solution contained 1 μM [Ca^{2+}] for outside-out patches and 0.2 μM [Ca^{2+}] for inside-out patches. At these concentrations, the effect of the β subunit on steady-state activation was minimized, while keeping the voltage range for channel activation at reasonable potentials (20–140 mV) [18]. The external face of the patch was continuously perfused with a high-potassium control saline.

For drug testing, Tx was added to this external control saline by 1:1000 to 1:100,000 dilutions from a 10 mM Tx stock dissolved in 100% DMSO. Final DMSO concentration did not exceed 0.1%, and this concentration of DMSO did not alter the biophysical properties of BK channels

when it was included in control saline without tamoxifen (data not shown). During recordings, patches were continuously and locally perfused by the experimental saline, using a gravity driven reservoir attached to a micromanifold (ALA Scientific, Westbury, NY). The manifold's outlet was placed 200 μm away and directly opposite the excised patch. In general, each patch was exposed to a control saline, 1 μM Tx, and then washed with the control saline. Additional concentrations of Tx were applied to the patch, with intermittent washes, until the seal was lost. All chemicals were obtained from Sigma unless otherwise indicated.

The number of channels per patch was determined by estimating the maximum patch conductance and dividing by an approximate single-channel conductance of 250 pS. Each patch contained between 1 and 100 BK channels. Even when a large number of channels were present, single-channel current amplitudes could be resolved with voltage pulses that produced low-open probabilities. From these single-opening events, current–voltage curves were generated and single-channel conductance was obtained from the slope of linear least-squares fits to these data. Transient and steady-state BK properties were determined from ensemble-averaged current recordings of 10–25 stimulus presentations. Leak currents were estimated at voltage steps that did not elicit channel activity and linearly subtracted off-line. Stray capacitance was minimal, but residual capacitance currents at the potassium equilibrium potential were fit with exponentials and piecewise linearly subtracted off-line so that fast-deactivation kinetics could be easily ascertained. In some cases, ensemble-averaged activation currents did not appear to reach saturation (see some intermediate steps in Fig. 2A). To determine if this could lead to erroneous conductance–voltage curves when using tail-current analysis, activation curves were fit with exponential curves and steady-state conductance–voltage relations were generated using steady-state current levels instead of tail-currents. First, steady-state current levels from these curve fits deviated less than 2% from peak currents reached at the end of the 100 ms voltage pulse (peak current = mean current from 95 to 100 ms). Second, conclusions based on tail-current *G–V* curves were supported by this alternative approach, and any error introduced by non-saturating activation curves was deemed minor.

Recordings were made with an Axopatch 200B amplifier, Digidata 1322A digitizer, and the pClamp 9.0 software suite (Axon Instruments, Foster City, CA). Data were sampled at 20 kHz and low-pass filtered at 5 kHz. Statistical analyses were performed using a Student's *t*-test with significance indicated by $p < 0.05$. Activation and deactivation kinetics were estimated with least-square fits to standard single-exponential curves in Clampfit, part of the pClamp software suite. Event idealization, estimation of open probability (NP_o), and determination of mean open dwell time for *N* channels were performed with the single-channel analysis tools in Clampfit. Averaged values are reported as means ± standard error of the mean. All recordings were made at room temperature (22–25 °C).

3. Results

3.1. Tamoxifen alters single-channel conductance

In previous reports, 1 μM Tx reduced the single-channel conductance of mammalian BK channels by 12–20% [24]. This effect was attributed to flickery block of the channel through interactions with the channel pore. Also, membrane impermeant forms of tamoxifen were less effective at reducing channel conductance when applied to the intracellular face of the channel, suggesting that channel block occurs through interaction with the extracellular portion of the channel [25]. Notably, the reduction in conductance was independent of co-assembly with β1. Fig. 1 shows Tx effects on single-channel gating of chicken BK channels, and salient features are illustrated in the current traces of Fig. 1A–C. Records in Fig. 1A were obtained from a membrane patch excised from a cell consisting of only pore-forming α subunits. At least four channels were present in this patch. In control saline, a holding potential of 60 mV elicited a slope conductance of 275 pS. When Tx was added to the control saline, single-channel conductance decreased to 262 pS in 1 μM Tx and 193 pS in 10 μM Tx. Open probability was relatively unchanged by 1 μM Tx, but was substantially reduced at the higher drug concentration, likely due to a concentration-dependent reduction in mean open time duration (4.68 ms in control saline, 3.39 ms in 1 μM Tx, 1.06 ms in 10 μM Tx; see Fig. 1B).

The reduction in single-channel conductance was also apparent in channels consisting of both α and cβ subunits. In Fig. 1C, unitary currents are shown for an inside-out patch exposed to 0.2 μM Ca^{2+} and held at 80 mV. Tamoxifen is lipophilic, and therefore capable of traversing the plasma membrane. The site of Tx and BK channel interaction (i.e. both gating energetics and conductance) appears to be at extracellular sites [25]. Therefore, when Tx is applied to inside-out patches, modulation of channel behavior is moderately delayed (∼2 min) compared to when Tx is applied to outside-out patches (<0.5 min). In Fig. 1C, channel open probability, single-channel conductance, and mean open duration were relatively unchanged immediately following the onset of 1 μM Tx application. After 2 min of local Tx perfusion, open probability increased and conductance and mean open duration decreased, supporting the notion that Tx acts at extracellular sites of avian BK subunits. From these exemplar traces, it appears that avian BK behavior mirrors that of mammalian homologs, with Tx reducing single-channel conductance regardless of co-assembly with cβ and

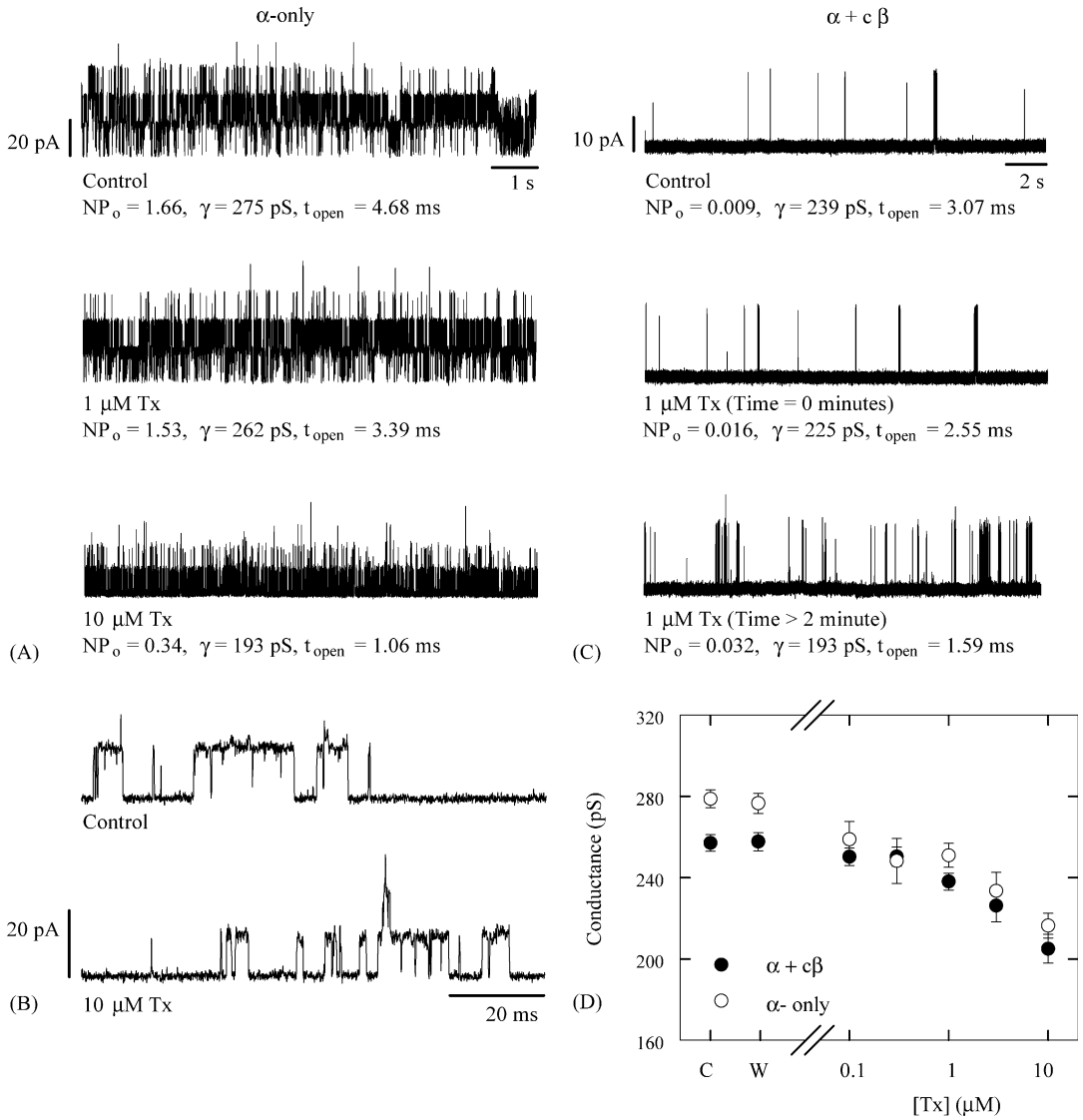

Fig. 1. Tamoxifen reduces single-channel conductance regardless of subunit composition. (A) Single-channel current traces are shown for an outside-out patch excised from an HEK293 cell transfected with α subunits alone. The patch was held at 60 mV and exposed to isometric potassium. The intracellular solution contained 1 μM [Ca^{2+}], and the extracellular face was locally perfused with either control saline (upper trace), 1 μM Tx (middle trace) or 1 μM Tx (lower trace). Open probability (NP_o) and mean open duration (t_{open}) were determined from event idealizations of 30 s recordings. Single-channel conductance was determined from unitary currents estimated from amplitude histograms. (B) High-time resolution records are shown for the patch in panel (A). (C) Single-channel currents are shown for an inside-out patch from an HEK cell transfected with α and cβ subunits. The patch was held at 80 mV, the intracellular solution contained 0.2 μM [Ca^{2+}], and the intracellular face was locally perfused with control saline (top trace) or 1 μM Tx. Currents were recorded for long durations and 10-s samples are shown for the beginning of the drug application (middle trace) and after more than 2 min of drug application (lower trace). Tx modulation of inside-out patches was delayed compared to outside-out patches, suggesting that the lipophilic compound had to traverse the membrane of inside-out patches and interact with extracellular binding sites. In panels (A–C), the lowest current level for each trace represents the closed state. (D) The averaged single-channel conductance is shown for outside-out patches from cells transfected with α-only (open circles) or α + cβ subunits (closed circles). Conductance values were obtained from linear-regression fits to single-channel current amplitudes at membrane voltages ranging from −50 to 140 mV. Baseline values were obtained in control saline before the application of tamoxifen (“C”). Tamoxifen reduced single-channel conductance in a concentration-dependent manner, but this effect was independent of subunit composition. Conductance returned to control values when patches were washed with control saline (“W”). The number of patches contributing to each data point varied between 6 and 14. Error bars indicate one standard error of the mean.

increasing channel open probability if α subunits are co-assembled with cβ.

Tamoxifen regulation of single-channel conductance was reversible and concentration dependent (Fig. 1D). Outside-out patches were stepped through a range of activation voltages, from −100 to 140 mV, and unitary current amplitudes could be resolved in multi-channel patches when open probability was low. Single-channel conductance was determined for each patch by the slope of linear, least-squares regression fits to current–voltage relations. Channels composed of α subunits alone had an average single-channel conductance of 278 ± 5 pS ($N = 11$) in control saline. This value decreased to 251 ± 7 pS (10% reduction, $p < 0.05$) in the presence of 1 μM Tx. Conductance returned to 277 ± 5 pS after the patches were returned to control saline, so the Tx effect

was completely reversible. For channels composed of α and cβ subunits, the average single-channel conductance was 257 ± 4 pS ($N = 14$) in control saline and 238 ± 4 pS in 1 μM Tx (7% reduction, $p < 0.05$). Upon washout of the drug, conductance returned to 258 ± 5 pS. There was no apparent rectification in current–voltage relations in the presence or absence of Tx, so this blocking effect was voltage independent. Concentrations of Tx above 1 μM were increasingly more effective at reducing single-channel conductance (Fig. 1D). Lower concentrations had no significant effect on α + cβ channels ($p > 0.05$), but had modest, yet significant effects on α-only channels ($p < 0.05$). Small differences in the effects of Tx on channels with and without cβ co-expression are possibly due to the small sample size and the estimation of conductance from short duration recordings. Nevertheless, these data confirm that the single-channel conductance of chicken BK channels is reduced in the presence of Tx, in a concentration dependent and reversible manner.

3.2. Tamoxifen shifts steady-state gating properties

In previous reports, the activation range of mammalian BK channels shifted to more negative potentials in the presence of Tx, and this effect was mediated through β1 subunits [24]. To test for similar effects on chicken BK channels, steady-state properties were assessed by tail-current analysis. Outside-out patches containing 1–100 BK channels were initially stepped from a holding potential of 0 to −50 mV, and this was followed by a series of steps to various activating voltages. Tail-currents were elicited by a final step to −40 mV. Since the patches contained relatively few BK channels, the stimulus was repeated for a total of 5–25 presentations, and the resulting currents were ensemble-averaged and leak subtracted off-line. Examples of ensemble-averaged traces are shown in Fig. 2A, and two important observations can be made. First, α + cβ channels showed slower activation and deactivation kinetics than channels consisting of α subunits alone. The slowing of channel kinetics is a general attribute of accessory β subunits [12,18]. Second, the presence of Tx caused a decrease in the maximum steady-state currents, and this was attributed, in part, to the reduction in single-channel conductance. Steady-state conductance–voltage (G–V) curves were constructed from tail-currents, and these curves were normalized by the peak conductance derived from Boltzman curve fits. Interestingly, the average reduction in single-channel conductance was significantly smaller than the reduction in maximum steady-state conductance ($p < 0.05$), when channels were exposed to 1 μM Tx compared with control saline (Fig. 2B). Therefore, Tx decreased the maximum open probability in addition to reducing single-channel conductance. This effect on maximum open probability is similar to that reported for another xenoestrogen, ICI-182,780 [32].

Steady-state conductance–voltage curves are shown in Fig. 2C for patches with α alone or α + cβ. In addition to effects on channel kinetics, β subunits generally increase the apparent calcium sensitivity of the BK channel, producing a leftward shift in the G–V curve and a more negative $V_{1/2}$. However, the half-activation voltage $V_{1/2}$ of α-only channels was similar to that for α + cβ channels, 63.8 ± 4.0 and 62.7 ± 2.8 mV, respectively. In a previous report, co-expression with the quail β subunit created BK channels with slower kinetics and a more negative $V_{1/2}$ at 1 μM Ca^{2+} [18]. However, differences between current and previous results lie primarily in the half-activation of α-only channels, not in the effects of the β subunit. The reason for this discrepancy is unknown and warrants further investigation. Nevertheless, the chicken homolog of the β subunit altered BK kinetics in a way that was similar to previous studies [12,18]. The half-activation voltage $V_{1/2}$ of α + cβ channels shifted to more negative potentials in the presence of 1 μM Tx ($\Delta V_{1/2} = 13.8 \pm 2.0$ mV), and this effect was statistically significant ($p < 0.05$) and reversible. In contrast, the $V_{1/2}$ of α-only channels shifted to the right in Tx ($\Delta V_{1/2} = -3.6 \pm 1.1$ mV), but while this change was statistically significant ($p < 0.05$), it was not fully reversible at this Tx concentration. It is also apparent from Fig. 2C that the rightward shift in α-only channels is primarily due to a change in Boltzman slope (i.e. a decrease in voltage sensitivity).

Concentration-dependent effects of Tx were investigated, and the results on steady-state properties are shown in Fig. 3. Conductance–voltage curves are shown for α-only channels in Fig. 3A. Half-activation shifted to more positive voltages, and this shift increased with increasing concentration of Tx (Fig. 3B). The change in $V_{1/2}$ was apparently due to a Tx effect on Boltzman slope (Fig. 3C). The change in slope and $V_{1/2}$ did not return to control values after the 1 μM Tx application was washed with control saline, and there was concern that this was due to drift in the biophysical properties of these channels over time. Since additional concentrations of Tx (0.1, 0.3, 3, 10 μM Tx) were applied in a random fashion, the concentration-dependent results in Fig. 3B and C, were not likely due to gradual, time-dependent changes in channel gating. Repeated washes with control saline after application of high-Tx concentrations showed a partial return of $V_{1/2}$ and Boltzman slope to control values, but changes to these parameters were not fully restored (data not shown).

The activation of BK channels co-assembled with cβ was similarly dependent on Tx concentration. Conductance–voltage curves for α + cβ channels show that activation by Tx is retained at higher drug concentrations, with the added effect of a decrease in voltage sensitivity (Fig. 3D). The change in half-activation voltage was fitted with a modified Hill equation, and this analysis gave an EC_{50} of 0.2 μM Tx (Fig. 3E). For concentrations of Tx at or below 1 μM, changes in the activation curve could be

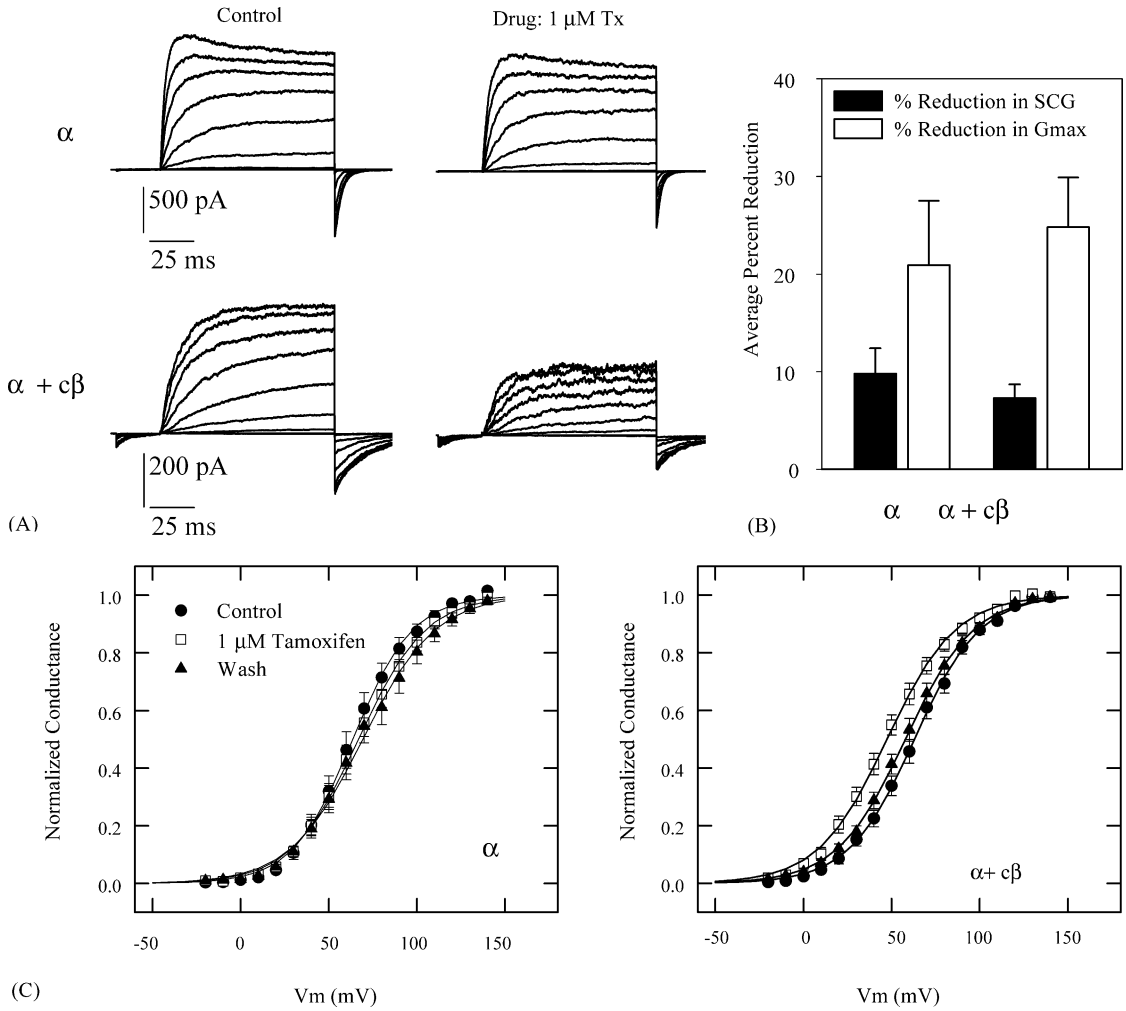

Fig. 2. Tamoxifen shifts activation to more negative potentials when α subunits are co-expressed with cβ. (A) Leak-subtracted activation currents are shown for exemplar outside-out patches from HEK cells transfected with α subunits alone (top panel series) or α and cβ subunits (bottom panel series). Patches were perfused with control saline (left panels) or 1 μM Tx in control saline (right panels). Current traces represent the average of 25 stimulus presentations. This stimulus consisted of an initial voltage step from a holding potential of 0 to −50 mV. Activation steps ranged from −20 to 140 mV and were followed by a final step to −40 mV. For these examples, current traces are shown for increments of 20 mV in voltage steps. (B) A comparison is made between the percent reduction in average single-channel conductance (SCG) (Fig. 1D) and the percent reduction in averaged maximum steady-state conductance G_{max} between 1 μM Tx and control saline. Sample sizes: α-only SCG (11) and G_{max} (15); α + cβ SCG (14) and G_{max} (13), (C) conductance–voltage (*G–V*) curves were constructed from tail-currents at −40 mV for the control, drug, and wash conditions in (A). The *G–V* curves from multiple patches were fit to Boltzman functions ($G = G_{max}/[1 + e^{zF(V_{1/2}-V)/RT}]$), and each curve was normalized by the maximum conductance level from the fits. The averaged *G–V* curves are shown for patches containing α-only ($N = 15$; left) and α + cβ ($N = 13$; right) subunits. Boltzman functions were also fit to the averaged curves. Fit parameters: for α-only, control $z = 1.48$, $V_{1/2} = 63.6$ mV, drug $z = 1.31$, $V_{1/2} = 66.8$ mV, wash $z = 1.22$, $V_{1/2} = 69.2$ mV; for α + cβ control, $z = 1.35$, $V_{1/2} = 62.9$ mV, drug $z = 1.29$, $V_{1/2} = 47.4$ mV, wash $z = 1.30$, $V_{1/2} = 57.9$ mV. Error bars indicate one standard error of the mean.

represented by a leftward shift, but for higher concentrations, the shape of the curve indicated that two processes were involved. While a change in the slope of the Boltzman fit was not apparent at lower Tx concentrations, there was a significant decrease in slope at 3 and 10 μM Tx ($p < 0.05$) (Fig. 3F). From these data, it is apparent that Tx alters both single-channel conductance and voltage sensitivity regardless of subunit composition. Net activation by Tx, however, is mediated through co-expression with cβ.

To further explore the mechanism of Tx modulation, conductance–voltage curves for channels in control saline or 1 μM Tx were fit with a voltage-dependent version of the Monod–Wyman–Changeux model for allosteric proteins [33]. This model, although simplified, has been used previously to describe BK channel properties and is capable of reproducing calcium and voltage dependence over a wide range of conditions [12,34]. According to the model, open probability (i.e. normalized conductance G/G_{max}) as a function of membrane voltage *V* and calcium concentration [Ca^{2+}] is given by:

$$P_o = \frac{1}{1 + \left\{\frac{1+[Ca^{2+}]/K_c}{1+[Ca^{2+}]/K_o}\right\}^4 L(0)\exp^{\frac{-QFV}{RT}}}, \quad (1)$$

where K_c and K_o are the calcium dissociation constants for closed and open states, respectively, $L(0)$ is the open closed

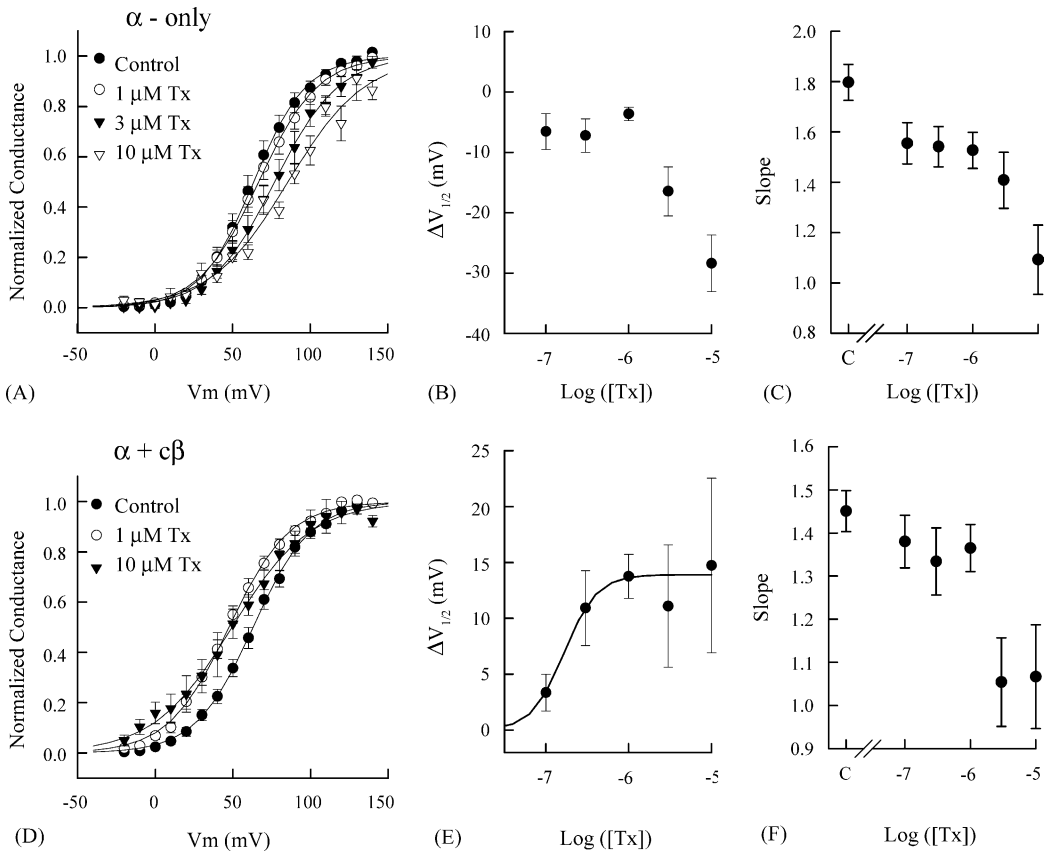

Fig. 3. Tamoxifen modulates BK channel behavior in a concentration-dependent manner. (A) *G–V* relations are shown for patches consisting of α subunits alone. Control and 1 μM Tx curves are repeated from Fig. 2B and are shown alongside similar curves for higher tamoxifen concentrations. Boltzman curve fits were used to estimate half-activation voltage and slope (i.e. voltage sensitivity) for each drug concentration. (B) The concentration-dependent shift in half-activation voltage $\Delta V_{1/2}$ is plotted for patches consisting of α subunits alone. Negative values indicate a rightward shift in half-activation. (C) The slope of the Boltzman curve fits are shown for patches consisting of α subunits alone. Tamoxifen reduced voltage sensitivity in a concentration-dependent fashion. Baseline values were obtained in control saline prior to drug application ("C"). Similar curves were generated for patches from HEK cells transfected with α and cβ subunits, including *G–V* curves (D), $\Delta V_{1/2}$ curves (E), and Boltzman slope curves (F). The $\Delta V_{1/2}$ of α + cβ patches was fit to a modified Hill equation $\Delta V_{1/2} = \Delta V_{max}/\{1 + 10^{((\log(EC_{50}-[Tx])\times n)}\}$, resulting in an EC_{50} of 0.2 μM tamoxifen and a Hill coefficient n of 2.2. As with α subunits alone, Tx reduced voltage sensitivity in a concentration-dependent fashion. Tested concentrations included 0.1, 0.3, 1, 3, and 10 μM Tx. Limited concentrations are presented in (A and D) for clarity, since curves are clustered together. Error bars in all panels indicate one standard error of the mean.

equilibrium constant in the absence of Ca^{2+} or applied voltage, Q is the gating charge at equilibrium, and the constant RT/F is approximately 25 mV at room temperature. A parametric analysis of Eq. (1) shows that K_c/K_o governs calcium affinity such that larger ratios increase the spacing between *G–V* curves produced by different calcium concentrations [12]. Placement of *G–V* curves along the voltage axis is largely governed by $L(0)$, whereas the slope of the *G–V* curve is defined by Q. Data in this report were collected with a single $[Ca^{2+}]$, so appropriate values of K_c and K_o had to be determined prior to curve fitting. For both α and α + cβ channels in control saline, values for K_c and K_o were held constant at 10 and 1 μM, respectively. These values were chosen because they give reasonable fits to data from mammalian isoforms [12]. Moreover, these values were held constant when fitting data from Tx-treated channels, since tamoxifen's effects on BK gating is apparently calcium independent [24]. The model was applied to data for both channel configuration in either control or 1 μM Tx salines (see Fig. 2C). From a comparison of Eq. (1) and the Boltzman function used to originally fit the data in Fig. 2C, it is easily shown that Boltzman slope z is equivalent to gating charge Q in the MWC model. It was shown in Fig. 3A–C that Tx caused a rightward shift in $V_{1/2}$ for channels composed of α subunits alone, and that this was due, in part, to a change in voltage sensitivity. Curve fits to the MWC model supported the conclusion that Tx caused a reduction in voltage sensitivity (i.e. gating charge), but they also revealed a reduction in the intrinsic energetics of channel opening (i.e. shift in $L(0)$). For α-only channels, $L(0)$ decreased from 470 in control saline to 367 in 1 μM Tx (22% reduction). Typically, a reduction in $L(0)$ results in a shift of the *G–V* curve to more negative potentials. However, this effect was accompanied by a reduction in gating charge from 1.48 in control saline to 1.37 in 1 μM Tx. Therefore, the net rightward shift in $V_{1/2}$ for these channels resulted from a reduction in gating charge and a reduction in the intrinsic energetics associated with the central conformational change between closed and open states. For channels composed of α and cβ subunits,

Tx also mediated reductions in Q and $L(0)$, but the net effect was fundamentally different than that observed with α-only channels. In this case, the reduction in Q was from 1.35 in control saline to 1.29 in 1 μM Tx, and the reduction in $L(0)$ was 62% from 329 in control saline to 125 in 1 μM Tx. The profound effect on conformational equilibrium resulted in a net leftward shift of the *G–V* curve in the presence of Tx. Using the MWC model, it appears that Tx mediates two primary effects on the voltage-dependent transitions between open and closed conformations, but the relative contribution of these two mechanisms to steady-state activation is modulated by the presence or absence of cβ.

3.3. Tamoxifen modulates channel kinetics

In most cases, excised patches contained multiple channels, making it difficult to draw conclusions about changes to channel kinetics from dwell times in open and closed states. However, activation and deactivation kinetics could be estimated from ensemble-averaged current traces, as in Fig. 2A. The regulatory properties of cβ were similar to the effects of quail β and bovine β1 [18,30], in that both activation and deactivation rates decreased in channels comprised of α + cβ compared with α subunits alone. For example, mean-activation time constants at +120 mV were 17.6 ± 1.8 and 4.0 ± 0.6 ms for channels with and without cβ, respectively. Cells putatively expressing α + cβ subunits were produced by transfection with separate plasmids for α and cβ. Therefore, it was possible that not all α expressing cells were co-assembled with cβ. While we are unable to quantitatively determine the stoichiometries of excised channels, the distributions of activation time constants for channels from cells with and without cβ were non-overlapping, suggesting that transfection with separate plasmids consistently produced heteromeric channels.

Changes in channel kinetics due to Tx were not readily apparent in the examples of Fig. 2A, but consistent effects were found when time constants were averaged from single-exponential fits to activation and deactivation transients. Activation time constants could be reliably fit to currents from voltage steps to 60–140 mV. Averaged values are shown for α-only channels in Fig. 4A, and curves in the presence or absence of Tx are overlapped. The forward gating charge q_f was calculated to determine the voltage dependence on activation rate. For the curves in

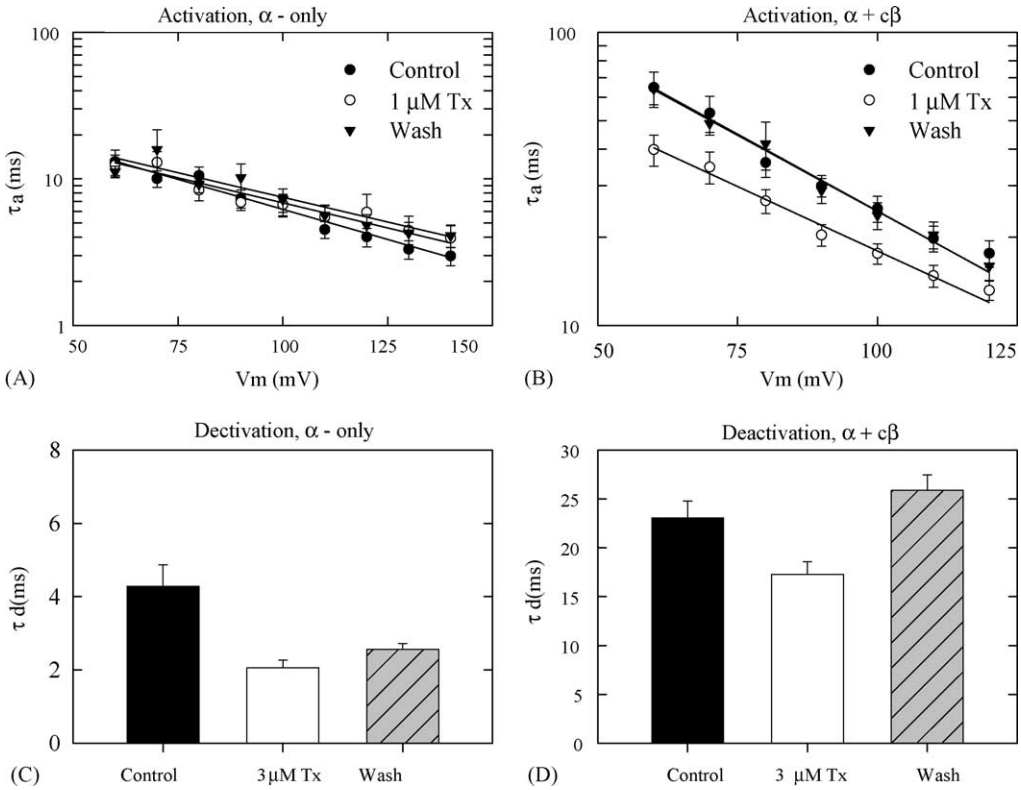

Fig. 4. Tamoxifen increases the activation rate of BK channels co-assembled with cβ subunits. (A and B) The macroscopic rate of channel activation τ_a was estimated from single-exponential fits to activation currents. Straight lines represent curve fits to $\tau_a = A\exp(-q_f FV/RT)$. The activation rates of α-only channels were unaffected by the drug (A), but activation rates increased when 1 μM Tx was perfused onto patches containing α + cβ subunits (B). (C and D) Average-deactivation time constants are shown for patches without (C) and with (D) cβ co-expression. The deactivation time constant for each patch was obtained by averaging time constants from single-exponential fits to five tail-current traces at −40 mV, where each trace was elicited by separate activation steps (140–100 mV). Time constants were then averaged across multiple patches to characterize the deactivation kinetics for channels with and with cβ subunits. Deactivation rates were faster when 3 μM Tx was present in the perfusate compared with control saline alone ($p < 0.05$), and this result was independent of co-expression with cβ subunits. Error bars in all panels indicate one standard error of the mean.

Fig. 4A, q_f was 0.49 ± 0.03, 0.41 ± 0.04, and 0.44 ± 0.04 for channels in control, 1 μM Tx, and wash conditions, respectively. There was no significant difference between control and drug conditions ($p > 0.05$). The activation rates for channels pulled from cells transfected with α and cβ are shown in Fig. 4B. For these channels, Tx increased activation rate at each voltage step. Gating charge decreased from a control value of 0.61 ± 0.05 to 0.46 ± 0.03 in the presence of 1 μM Tx, and this decrease was statistically significant ($p < 0.05$). Upon washout of the drug with control saline, gating charge returned to 0.57 ± 0.03, and this value was not statistically different from the control value ($p > 0.05$). Therefore, tamoxifen's action on activation kinetics was two-fold. First, Tx-mediated voltage-dependent changes in channel kinetics through a reduction in gating charge, and this effect may be independent of cβ co-expression. This change in forward gating charge q_f presumably reflects the reduction in steady-state gating charge or Boltzman slope, shown in Fig. 3C and F. Second, Tx increased the activation rate for α + cβ channels, reflecting a reduction in the energy barrier for transitions from closed to open states.

The rate of channel deactivation also was investigated. In a preliminary analysis, deactivation rates were obtained from tail-currents generated at −40 mV from a single-activation pre-pulse of 100 mV. For channels with and without cβ, deactivation rate decreased in the presence of 1 μM Tx, but differences in the means of control and Tx salines were not significant ($p > 0.05$). This result was surprising given the observation that Tx (Fig. 1A–C) and other (xeno)estrogens [32] destabilize the bursting open state. However, variance in the averaged-deactivation rates may have hidden Tx effects on this kinetic parameter. Since BK channel gating is generally modeled with discrete-state Markovian processes [35,36], it is legitimate to assume that deactivation rates at −40 mV are independent of the pre-pulse from which tail-currents were elicited. In Fig. 4, deactivation time constants were averaged from tail-currents elicited by multiple-activation pulses (five pulses between 140 and 100 mV), and these were combined for channels without (Fig. 4C) and with (Fig. 4D) cβ co-expression. Paired Student's *t*-tests revealed significant differences in mean-deactivation rates between control and 3 μM Tx salines, regardless of cβ co-expression ($p < 0.05$). Kinetic effects were concentration dependent so the higher Tx concentration used in this analysis (3 μM) was chosen to clearly reveal modulation of channel deactivation. Therefore, Tx increased the rate of deactivation, but in contrast to effects on activation kinetics, the modulation of deactivation was independent of channel composition.

4. Discussion

Many reports have established (xeno)estrogen sensitivity in mammalian BK channels, with channel activation occurring through both β1 and β4 subunits [22–24,26,37]. The results in this paper extend this sensitivity to the putative chicken β homolog. The features and magnitude of effects on avian and mammalian channels were comparable [24]. Similarities included a reduction in single-channel conductance regardless of subunit composition and activation by Tx in the presence of the cβ subunit. However, the mechanism for Tx modulation remains unknown. One prevailing view is that Tx interacts with extracellular binding sites on as yet unidentified components of the BK complex or on the α and β subunits themselves [25]. In this model, Tx reduces single-channel conductance by binding to the BK channel pore and activates the channel possibly through direct binding to the β subunit.

To identify conserved residues that may act as interaction domains, we aligned the amino acid sequences for chick β and human β1–β4 (Fig. 5A). The topologies of the avian and mammalian subunits are highly conserved. Common features include two transmembrane domains, intracellular ends, a large extracellular loop, four conserved extracellular cysteine residues, and a common extracellular *N*-linked glycosylation site. However, sequence diversity is high (Fig. 5B), with percent identity ranging from 22 (β1–β4) to 46% (β1–cβ). In Fig. 5A, conserved residues between cβ, β1, and β4 are boxed in black. Only 32 residues were conserved, reflecting less than 16% identity among these proteins. Of the conserved residues, 24 (85%) were also common to human β2 and β3. Inspection of Fig. 5A reveals the greatest commonalities around four cysteines, which likely govern folding of the extracellular loop [14]. Potential binding motifs may be limited to conserved residues in the vicinity of these four cysteines. By investigating the functional effects of these domains, we may identify unique (xeno)estrogen binding motifs. Alternatively, if specific binding sites are not present in these domains, we may conclude that interaction occurs through other indirect mechanisms.

Data in this paper address the mechanisms of single-channel block and channel activation by analogy to lipid-mediated changes to channel properties. Previous reports have suggested a flickery block mechanism for altering single-channel conductance [24]. Flickery block is characterized by brief transitions that produce noisy open-state currents and an apparent reduction in channel conductance. The traces in Fig. 1B show clear open-state plateaus, without increased noise in the open state (S.D. = 1.09 in control saline; S.D. = 1.28 in 10 μM Tx). While these results cannot rule out extremely fast flickery block, other possibilities must be considered, with a mind to guide future investigations. There is a growing appreciation for the influence of lipid content and bilayer mechanics on channel properties, including single-channel conductance and gating kinetics [38,39]. In fact, Tx-mediated changes in conductance and deactivation kinetics were reminiscent of reported cholesterol effects [40], where a substantial increase in cholesterol content reduced both channel mean

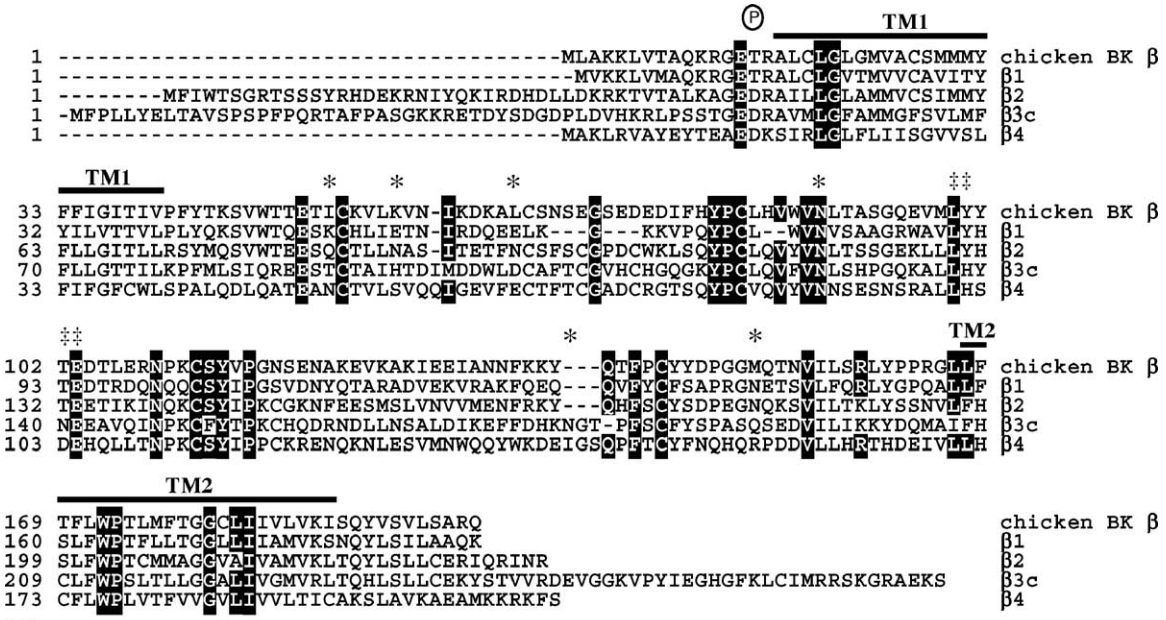

(A)

Percent Identity					
1	2	3	4	5	
	46.1	45.5	29.5	27.0	1, chicken BK β
		44.0	30.4	21.5	2, β1
			36.6	30.5	3, β2
				29.5	4, β3c
					5, β4

(B)

Fig. 5. Sequence alignment for mammalian and avian β subunits. (A) The open reading frame of the chicken BK channel β subunit is compared with the human β subunits β1–β4. Human sequences were aligned according to Behrens et al. and compared with the chicken sequence using DNAStar and the ClustalW algorithm. Identical amino acids among cβ, β1, and β4 are boxed in black. Identical residues in β2 and β3 also are boxed in black. Gaps in the sequence alignment are indicated by dashes. Solid black lines indicate putative transmembrane domains, TM1 and TM2, based on a hydrophobicity plot of the chicken β sequence. Consensus *N*-glycosylation sites are marked for all sequences (asterisks at respective asparagines residues). Residues associated with high-affinity charybdotoxin binding to β1 are indicated (‡). A PKC phosphorylation site is shared between chicken β and β1 at the intracellular NH2 terminus (circled P). Accession numbers are as follows: chicken β subunit, AF077369; β1, AY044441; β2, AF099137; β3c, AF139471; and β4, AF207992. (B) The percent identity is shown for pairwise comparisons of each sequence in (A).

open time and single-channel conductance. It is possible that the amphipathic nature of tamoxifen could act through mechanical changes to the surrounding bilayer rather than directly binding to the channel pore.

Increases in cholesterol content reduced mean open time by reducing the energetics of transition from open to closed states [40]. Similar observations have been reported for BK channels in coronary endothelial cells, where the xenoestrogen ICI-182,780 also shortened the mean open-state dwell time. Since coronary endothelial cells consist of α subunits alone [41], the effect of Tx on channel deactivation was independent of β subunit co-expression, much like the reported effects on single-channel conductance. We observed a similar destabilization of the open state (Fig. 2A–C), even though this parameter was not quantified. By facilitating transitions from open to closed states, drug application should result in accelerated-deactivation kinetics. This notion is supported by the current data set, where deactivation increased in the presence of Tx, regardless of cβ co-expression. Therefore, (xeno)estrogen modulation of BK channel kinetics is conserved among avian and mammalian isoforms and can be extended to include both Tx and ICI-182,780. Moreover, these effects occur through interaction with α subunits alone, possibly by changing the mechanical stresses in the membrane bilayer rather than directly binding to the channel itself.

Tamoxifen modulation of α-only channels was also manifested in steady-state gating properties. Previously, it was concluded that Tx had little effect on the gating properties of α-only channels, beyond reductions in single-channel conductance [24]. The present results, however, show a concentration-dependent reduction in voltage sensitivity that was independent of co-expression with cβ. Studies on mammalian isoforms were limited to 1 μM Tx, where the effect on voltage sensitivity may have been too small to resolve. In order to further explore the mechanism of interaction with the α subunits, steady-state *G–V* curves were fit to a voltage-dependent MWC model. In this way, we could determine whether Tx modulation was restricted to reductions in voltage sensitivity (i.e. gating charge *Q*). Interestingly, model fits to α-only data demonstrated an unexpected reduction in the equilibrium constant *L*(0). In

general, reductions in this parameter result in a leftward shift in the *G–V* curves [12]. However, the net effect of reductions in *Q* and *L*(0) resulted in voltage-dependent inhibition of α-only channels. For BK channels composed of α + cβ, the profound reduction in *L*(0) resulted in a net leftward shift of *G–V* or activation. Therefore, Tx modulation of α-only and α + cβ channels was dependent on the relative contributions of two gating mechanisms. This model supports the idea that Tx mediates its effects through conformational changes to the α subunit alone, instead of direct binding to the β subunit. These results are supported by recent evidence demonstrating low-affinity binding of estradiol to α subunits [42]. The estradiol to α subunit interaction was facilitated by co-expression with β, but the results did not support direct binding of estradiol to β subunits [42].

In addition to addressing potential interaction mechanisms, the current data resolve an apparent discrepancy in (xeno)estrogen effects on activation kinetics. In human channels heterologously expressed in oocytes, 17β-estradiol accelerated the kinetics of BK channels comprised of α and β1 subunits [22]. It was surprising that Tx had no effect on the activation kinetics of BK channels from canine smooth muscle, since these channels most likely included α and β1 subunits [24]. The discrepancy between Tx effects on the activation of avian and mammalian channels may result from different recording conditions. In Fig. 4B, activation rate increased with membrane voltage, but Tx-mediated changes in gating charge reduced the steepness of this relationship. As a result, tamoxifen's effect on activation rate was less pronounced at more positive membrane voltages. Since results from canine smooth muscle cells were obtained at 150 mV in 100 nM [Ca^{2+}], differences in channel kinetics may have been obscured.

Acknowledgements

The author thanks Dr. Paul A. Fuchs for helpful comments on earlier drafts of this manuscript. This work was supported by grants from the National Institute of Deafness and Communication Disorders (no. DC00276 to P.A. Fuchs, training grant no. T32 00023, and core grant no. P30 DC 05188).

References

[1] Robitaille R, Charlton MP. Presynaptic calcium signals and transmitter release are modulated by calcium-activated potassium channels. J Neurosci 1992;12:297–305.
[2] Pattillo JM, Yazejian B, DiGregorio DA, Vergara JL, Grinnell AD, Meriney SD. Contribution of presynaptic calcium-activated potassium currents to transmitter release regulation in cultured Xenopus nerve-muscle synapses. Neuroscience 2001;102:229–40.
[3] Fettiplace R, Fuchs PA. Mechanisms of hair cell tuning. Annu Rev Physiol 1999;61:809–34.
[4] Liu YC, Patel HJ, Khawaja AM, Belvisi MG, Rogers DF. Neuroregulation by vasoactive intestinal peptide (VIP) of mucus secretion in ferret trachea: activation of BK(Ca) channels and inhibition of neurotransmitter release. Br J Pharmacol 1999;126:147–58.
[5] Herrera GM, Nelson MT. Differential regulation of SK and BK channels by Ca(2+) signals from Ca(2+) channels and ryanodine receptors in guinea-pig urinary bladder myocytes. J Physiol 2002;541:483–92.
[6] Wu SN. Large-conductance Ca2+-activated K+ channels: physiological role and pharmacology. Curr Med Chem 2003;10:649–61.
[7] Orio P, Rojas P, Ferreira G, Latorre R. New disguises for an old channel: Maxi-K channel beta-subunits. News Physiol Sci 2002;17:156–61.
[8] Xia X, Hirschberg B, Smolik S, Forte M, Adelman JP. dSLo interacting protein 1, a novel protein that interacts with large-conductance calcium-activated potassium channels. J Neurosci 1998;18:2360–9.
[9] Schopperle WM, Holmqvist MH, Zhou Y, Wang J, Wang Z, Griffith LC, et al. Slob, a novel protein that interacts with the Slowpoke calcium-dependent potassium channel. Neuron 1998;20:565–73.
[10] Ling S, Sheng JZ, Braun JE, Braun AP. Syntaxin 1A co-associates with native rat brain and cloned large conductance, calcium-activated potassium channels in situ. J Physiol 2003;553:65–81.
[11] Ji J, Salapatek AM, Lau H, Wang G, Gaisano HY, Diamant NE. SNAP-25, a SNARE protein, inhibits two types of K channels in esophageal smooth muscle. Gastroenterology 2002;122:994–1006.
[12] Cox DH, Aldrich RW. Role of the beta1 subunit in large-conductance Ca(2+)-activated K(+) channel gating energetics. Mechanisms of enhanced Ca(2+) sensitivity. J Gen Physiol 2000;116:411–32.
[13] Garcia-Valdes J, Zamudio FZ, Toro L, Possani LD, Possan LD. Slotoxin, alphaKTx1.11, a new scorpion peptide blocker of Maxi-K channels that differentiates between alpha and alpha+beta (beta1 or beta4) complexes. FEBS Lett 2001;505:369–73.
[14] Hanner M, Vianna-Jorge R, Kamassah A, Schmalhofer WA, Knaus HG, Kaczorowski GJ, et al. The beta subunit of the high conductance calcium-activated potassium channel. Identification of residues involved in charybdotoxin binding. J Biol Chem 1998;273:16289–96.
[15] McManus OB, Helms LM, Pallanck L, Ganetzky B, Swanson R, Leonard RJ. Functional role of the beta subunit of high conductance calcium-activated potassium channels. Neuron 1995;14:645–50.
[16] Jiang Z, Wallner M, Meera P, Toro L. Human and rodent Maxi-K channel beta-subunit genes: cloning and characterization. Genomics 1999;55:57–67.
[17] Oberst C, Weiskirchen R, Hartl M, Bister K. Suppression in transformed avian fibroblasts of a gene (CO6) encoding a membrane protein related to mammalian potassium channel regulatory subunits. Oncogene 1997;14:1109–16.
[18] Ramanathan K, Michael TH, Fuchs PA. Beta subunits modulate alternatively spliced, large conductance, calcium-activated potassium channels of avian hair cells. J Neurosci 2000;20:1675–84.
[19] Song J, Standley PR, Zhang F, Joshi D, Gappy S, Sowers JR, et al. Tamoxifen (estrogen antagonist) inhibits voltage-gated calcium current and contractility in vascular smooth muscle from rats. J Pharmacol Exp Ther 1996;277:1444–53.
[20] Pedram A, Razandi M, Aitkenhead M, Hughes CC, Levin ER. Integration of the non-genomic and genomic actions of estrogen. Membrane-initiated signaling by steroid to transcription and cell biology. J Biol Chem 2002;277:50768–75.
[21] Henriquez M, Riquelme G. 17beta-estradiol and tamoxifen regulate a maxi-chloride channel from human placenta. J Membr Biol 2003;191:59–68.
[22] Valverde MA, Rojas P, Amigo J, Cosmelli D, Orio P, Bahamonde MI, et al. Acute activation of Maxi-K channels (hSlo) by estradiol binding to the beta subunit. Science 1999;285:1929–31.
[23] Dick GM. The pure anti-oestrogen ICI 182,780 (Faslodex) activates large conductance Ca(2+)-activated K(+) channels in smooth muscle. Br J Pharmacol 2002;136:961–4.

[24] Dick GM, Rossow CF, Smirnov S, Horowitz B, Sanders KM. Tamoxifen activates smooth muscle BK channels through the regulatory beta 1 subunit. J Biol Chem 2001;276:34594–9.
[25] Dick GM, Hunter AC, Sanders KM. Ethylbromide tamoxifen, a membrane-impermeant antiestrogen, activates smooth muscle calcium-activated large-conductance potassium channels from the extracellular side. Mol Pharmacol 2002;61:1105–13.
[26] Behrens R, Nolting A, Reimann F, Schwarz M, Waldschutz R, Pongs O. hKCNMB3 and hKCNMB4, cloning and characterization of two members of the large-conductance calcium-activated potassium channel beta subunit family. FEBS Lett 2000;474:99–106.
[27] Amberg GC, Bonev AD, Rossow CF, Nelson MT, Santana LF. Modulation of the molecular composition of large conductance, Ca(2+) activated K(+) channels in vascular smooth muscle during hypertension. J Clin Invest 2003;112:717–24.
[28] Duncan RK, Fuchs PA. Variation in large-conductance, calcium-activated potassium channels from hair cells along the chicken basilar papilla. J Physiol 2003;547:357–71.
[29] Welshons WV, Wolf MF, Murphy CS, Jordan VC. Estrogenic activity of phenol red. Mol Cell Endocrinol 1988;57:169–78.
[30] Ramanathan K, Michael TH, Jiang GJ, Hiel H, Fuchs PA. A molecular mechanism for electrical tuning of cochlear hair cells. Science 1999;283:215–7.
[31] Jiang GJ, Zidanic M, Michaels RL, Michael TH, Griguer C, Fuchs PA. CSlo encodes calcium-activated potassium channels in the chick's cochlea. Proc R Soc Lond Ser B Biol Sci 1997;264:731–7.
[32] Liu YC, Lo YC, Huang CW, Wu SN. Inhibitory action of ICI-182,780, an estrogen receptor antagonist, on BK(Ca) channel activity in cultured endothelial cells of human coronary artery. Biochem Pharmacol 2003;66:053–63.
[33] Monod J, Wyman J, Changeux JP. On the nature of allosteric transitions: a plausible model. J Mol Biol 1965;12:88–118.
[34] Cox DH, Cui J, Aldrich RW. Allosteric gating of a large conductance Ca2+-activated K+ channel. J Gen Physiol 1997;110:257–81.
[35] Silberberg SD, Lagrutta A, Adelman JP, Magleby KL. Wanderlust kinetics and variable Ca(2+)-sensitivity of dSlo, a large conductance Ca(2+)-activated K+ channel, expressed in oocytes. Biophys J 1996;71:2640–51.
[36] Rothberg BS, Magleby KL. Gating kinetics of single large-conductance Ca2+-activated K+ channels in high Ca2+ suggest a two-tiered allosteric gating mechanism. J Gen Physiol 1999;114:93–124.
[37] Dick GM, Sanders KM. (Xeno)estrogen sensitivity of smooth muscle BK channels conferred by the regulatory beta1 subunit: a study of beta1 knockout mice. J Biol Chem 2001;276:44835–40.
[38] Park JB, Kim HJ, Ryu PD, Moczydlowski E. Effect of phosphatidylserine on unitary conductance and Ba2+ block of the BK Ca2+-activated K+ channel: re-examination of the surface charge hypothesis. J Gen Physiol 2003;121:375–97.
[39] Yuan C, O'Connell RJ, Feinberg-Zadek PL, Johnston LJ, Treistman SN. Bilayer thickness modulates the conductance of the BK channel in model membranes. Biophys J 2004;86:3620–33.
[40] Chang HM, Reitstetter R, Mason RP, Gruener R. Attenuation of channel kinetics and conductance by cholesterol: an interpretation using structural stress as a unifying concept. J Membr Biol 1995;143:51–63.
[41] Papassotiriou J, Kohler R, Prenen J, Krause H, Akbar M, Eggermont J, et al. Endothelial K(+) channel lacks the Ca(2+) sensitivity-regulating beta subunit. FASEB J 2000;14:885–94.
[42] Korovkina VP, Brainard AM, Ismail P, Schmidt TJ, England SK. Estradiol binding to Maxi-K channels induces their down-regulation via proteasomal degradation. J Biol Chem 2004;279:1217–23.